INTERNATIONAL JOURNAL OF CIRCUIT THEORY AND APPLICATIONS
Int. J. Circ. Theor. Appl. 2008; **36**:493–509
Published online 20 August 2007 in Wiley InterScience (www.interscience.wiley.com). DOI: 10.1002/cta.442

LETTER TO THE EDITOR

The CCII+ and the ICCII as basic building blocks in low-pass filter realizations

Ahmed M. Soliman*, †

Electronics and Communication Engineering Department, Faculty of Engineering, Cairo University, Giza, Egypt

SUMMARY

Three new grounded capacitor current mode low-pass filters using two inverting second-generation current conveyor (ICCII) or one double output ICCII are given. The circuits employ the minimum number of passive circuit components, namely two resistors and two capacitors. The circuits are generated from three new voltage mode low-pass filters realized with the ICCII. A new grounded capacitor CCII+ current mode low-pass filter is generated from one of the new voltage mode low-pass filters employing two ICCII−. A new grounded passive component low-pass filter with independent control on Q and using three ICCII+ is also introduced. Spice simulation results based on using the 0.5 μm CMOS model are included to support the theoretical analysis. Copyright © 2007 John Wiley & Sons, Ltd.

Received 31 October 2006; Revised 26 June 2007; Accepted 7 July 2007

KEY WORDS: current conveyors; inverting current conveyors; low-pass filters; circuit transformations

1. INTRODUCTION

Since Sedra and Smith [1] introduced the second-generation current conveyor (CCII), it has been proved to be a very useful building block in active circuits. The inverting second-generation current conveyor (ICCII) was introduced in [2] as a new block to be added to the current conveyor family. The ICCII is considered to be a special case from the differential voltage current conveyor (DVCC) introduced independently in [3, 4] with a single Y input only. This active element can be easily implemented with CMOS technology as given in [2–4]. Fully differential current conveyors, FDCCII, have also been introduced in the literature and realized also in CMOS technology [5, 6]. Other types of current conveyors as well as voltage conveyors have also been defined [7, 8].

*Correspondence to: Ahmed M. Soliman, Electronics and Communication Engineering Department, Faculty of Engineering, Cairo University, Giza, Egypt.
†E-mail: asoliman@idsc.net.eg

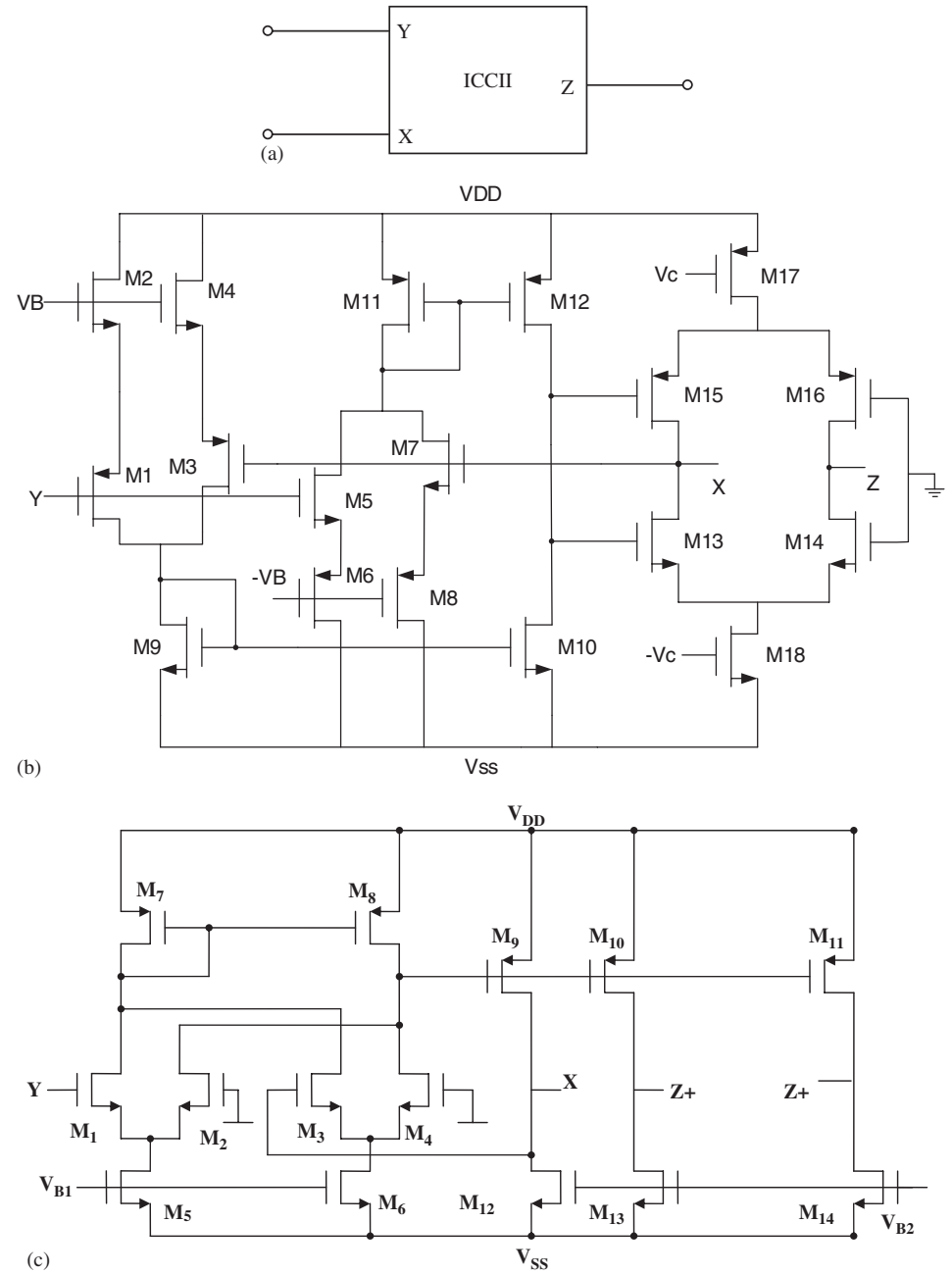

Figure 1. (a) Block diagram of ICCII; (b) the CMOS realization of the ICCII− given in [2]; and (c) the CMOS realization of the ICCII++ given in [3].

DOI: 10.1002/cta

The symbolic representation of the ICCII is shown in Figure 1(a). The relationship between terminal voltages and currents is given by [2]

$$\begin{pmatrix} I_y \\ V_x \\ I_z \end{pmatrix} = \begin{pmatrix} 0 & 0 & 0 \\ -B & 0 & 0 \\ 0 & \pm K & 0 \end{pmatrix} \begin{pmatrix} V_y \\ I_x \\ V_z \end{pmatrix} \tag{1}$$

In the ideal case $B = K = 1$ and the voltage at terminal X is the inversion of the voltage at terminal Y. The current at terminal Z follows the current at terminal X in magnitude, and the $\pm$ sign specifies the type of the current conveyor (ICCII+ or ICCII−). By convention, the positive sign is taken to mean that the currents at the X and Z terminals are both flowing inwards to the conveyor.

The important advantage of the ICCII is to obtain and design current mode circuits from their voltage mode counterparts using the adjoint network theorem [9, 10].

Several current mode filters using CCII and the minimum number of passive circuit components, namely two resistors plus two capacitors were introduced in the literature [11–14]. The circuit in [11] uses three two-output CCII. The circuit in [12] has two floating capacitors and the circuit in [13] has one floating capacitor. Besides the circuits reported in [12–14] suffer from the frequency-dependent non-zero input impedance. Also the circuits in [11, 14] have the output currents flowing in grounded capacitors; to use these currents additional current followers are needed and the capacitors are no longer grounded.

Circuit configurations employing only grounded capacitors [15, 16] are very attractive and are desirable for integrated circuit technology; owing to the parasitic capacitors the surrounding capacitors can be easily self-compensated as they are now in parallel with the grounded capacitors.

In this paper three new grounded capacitor current mode low-pass filters using two ICCII− and one new two single output CCII+ are generated from three new voltage mode circuits employing ICCII. All these circuits employ two resistors and two grounded capacitors and have identical transfer functions. An all grounded passive circuit component low-pass filter with independent control on Q and using three ICCII+ is also introduced.

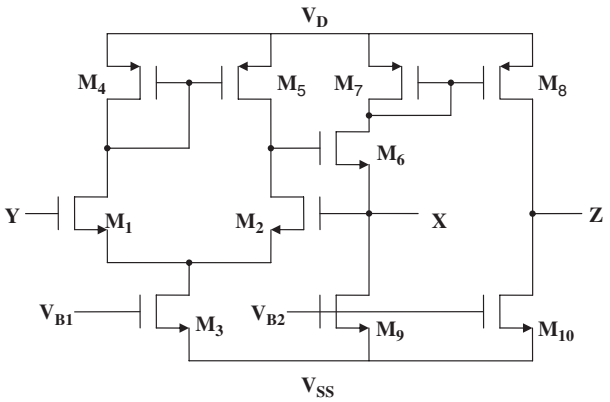

Figure 2. The CMOS realization of the CCII+ given in [17].

DOI: 10.1002/cta

Table I. Transistor aspect ratios of the ICCII− shown in Figure 1(b).

Transistor	W (μm)/L (μm)
$M_1, M_2, M_3, M_4, M_5, M_6, M_7, M_8$	50/1.5
M_9, M_{10}	12.5/1.5
M_{11}, M_{12}	37.5/1.5
M_{13}, M_{14}	25/0.5
M_{15}, M_{16}	50/0.5
M_{17}	82.5/1.5
M_{18}	39.5/1.5

Table II. Transistor aspect ratios of the ICCII++ shown in Figure 1(c).

Transistor	W (μm)/L (μm)
M_1, M_2, M_3, M_4	25/0.5
M_5, M_6	8/0.5
M_7, M_8	10/0.5
M_9, M_{10}, M_{11}	40/2
M_{12}, M_{13}, M_{14}	20/2.5

Table III. Transistor aspect ratios of the CCII+ shown in Figure 2.

Transistor	W (μm)/L (μm)
M_1, M_2	20/1
M_3	50/2.5
M_4, M_5	60/2.5
M_6	40/0.5
M_7, M_8	20/2.5
M_9, M_{10}	20/2.5

The Spice simulation results given in this paper are based on using the CMOS ICCII− shown in Figure 1(b) [2] and the CMOS ICCII++ circuit shown in Figure 1(c) [3] and CMOS CCII+ circuit shown in Figure 2 [17]. The transistor aspect ratios of these three circuits are given in Tables I–III based on the 0.5 μm CMOS model from MOSIS.

2. THE SINGLE ICCII LOW-PASS FILTER

The first ICCII+ minimum passive component low-pass filter given in this paper is generated from an operational amplifier (op amp)-based low-pass filter. It is of interest to review briefly the minimal component low-pass filters using op amps. Figure 3(a) represents the well-known Sallen–Key low-pass filter [18] employing the op amp as a unity gain non-inverting amplifier.

DOI: 10.1002/cta

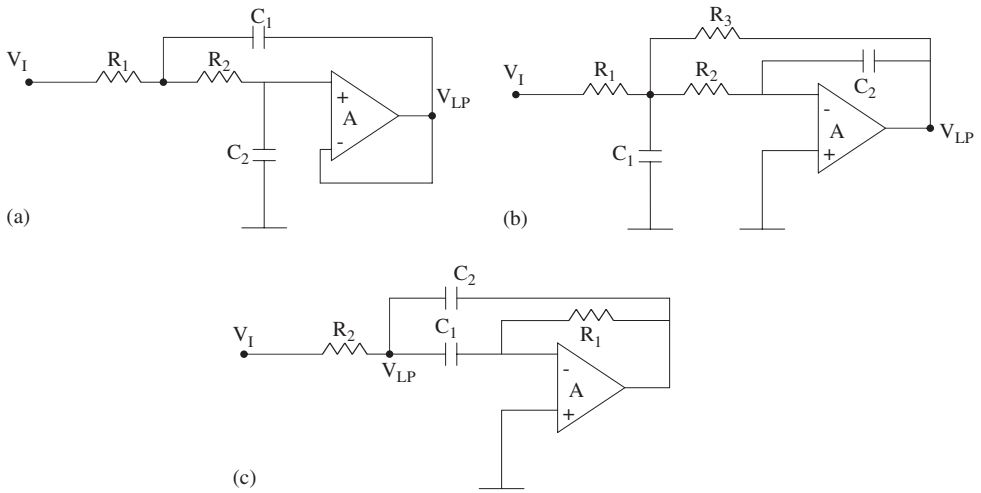

Figure 3. (a) Sallen–Key low-pass filter using unity gain amplifier [18]; (b) the multiple feedback single op amp low-pass filter [18]; and (c) the minimum passive component multiple feedback single op amp low-pass filter.

Table IV. Fractional shifts in ω_0 and Q of op amp and ICCII low-pass filters.

Circuit				
Active element	Figure	Numerator of transfer function	$\frac{\Delta\omega_0}{\omega_0}$	$\frac{\Delta Q}{Q}$
Op amp	3(a)	ω_0^2	$-Q(\frac{\omega_0}{\omega_t})$	$Q(\frac{\omega_0}{\omega_t})$
Op amp	3(b)	ω_0^2	$-Q(\frac{3\omega_0}{2\omega_t})$	$Q(\frac{\omega_0}{2\omega_t})$
Op amp	3(c)	$(\omega_0^2[1+\frac{s}{\omega_t}(1+\frac{2Qs}{(\omega_0)})])$	$-Q(\frac{\omega_0}{\omega_t})$	$Q(\frac{\omega_0}{\omega_t})$
ICCII+	4(b)	$K_0 B_0 \omega_0^2$	0	$\frac{\omega_0}{\omega_P} Q$
ICCII−	4(c)	$B[1+sC_2R_1(1-K)]\omega_0^2$	$-\frac{\omega_0}{\omega_1} Q$	$\frac{\omega_0}{\omega_1} Q$
ICCII+	5(a)	$K_0 B_0 \omega_0^2$	0	$\frac{\omega_0}{\omega_P} Q$
Two ICCII−	9(a)	$K_{0_1} K_{0_2} B_{0_2} \omega_0^2$	0	$\frac{\omega_0}{\omega_P} Q$

Its transfer function is given by

$$\frac{V_{\mathrm{LP}}}{V_i} = \frac{1}{s^2 C_1 C_2 R_1 R_2 + s(R_1 + R_2)C_2 + 1} \tag{2}$$

Of course this circuit has one floating capacitor and has limitations on the maximum frequency of operation based on the pole of the amp [19, 20] as will be summarized in Table IV based on the equal R design which is the recommended design of this circuit.

DOI: 10.1002/cta

The multiple feedback single op amp low-pass filter which employs three resistors plus two capacitors with one of them floating is shown in Figure 3(b). It has frequency limitation equations different from the circuit of Figure 3(a) as shown in Table IV [19, 20]. This is the well-known inverting low-pass filter, which is non-minimal in the passive circuit components and is included here just to complete the brief review of the single op amp low-pass filters. Another single op amp minimal passive component low-pass filter is shown in Figure 2(c). It is in fact the well-known low output impedance band-pass filter [17], but as a low-pass the output node is within the circuit as shown in Figure 3(c). The transfer function of the circuit is given by

$$\frac{V_{\mathrm{LP}}}{V_i} = \frac{1}{s^2 C_1 C_2 R_1 R_2 + s(C_1 + C_2)R_2 + 1} \tag{3}$$

The proper design for this circuit resulting in minimum passive sensitivities is the equal C design and the frequency limitation equations for this circuit [20, 21] are identical to those of the circuit of Figure 3(a) as shown in Table IV. The op amp single pole model, however, affects the numerator of the transfer function as seen in Table IV, which in turn affects the frequency response as will be evident from the Spice simulation results.

Now, consider the transformation of the op amp minimum passive components low-pass filters, to a current conveyor circuits. It is seen that the circuit of Figure 3(a) can be used with the CCII+ acting as a voltage buffer between ports Y and X. The CCII+ low-pass filter will still have one floating capacitor as in Figure 3(a). Now considering the circuit of Figure 3(c), it is seen that the input admittance of the circuit at the low-pass node is a parallel frequency-dependent negative resistance (FDNR) and a capacitor as shown in Figure 4(a). This parallel FDNR–C circuit is

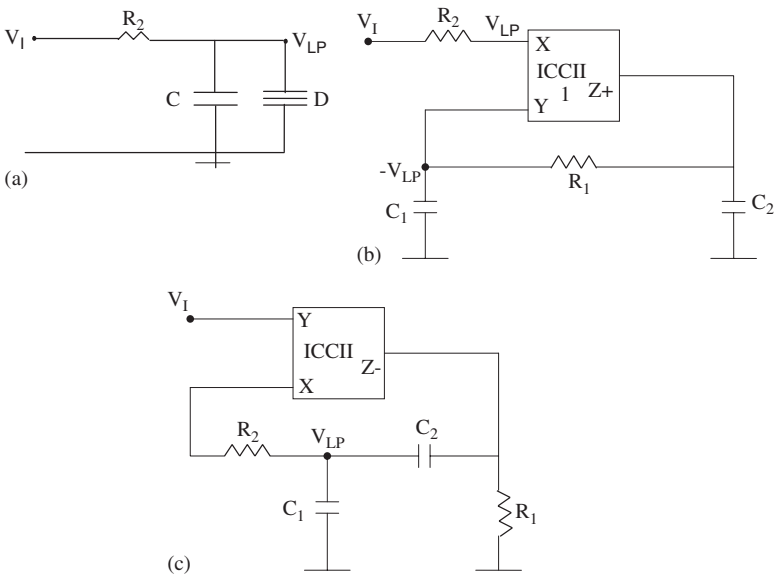

Figure 4. (a) The active RCD low-pass filter obtained from Figure 3(c); (b) grounded C voltage mode low-pass filter using a single ICCII+; and (c) high input impedance voltage mode low-pass filter using a single ICCII−.

DOI: 10.1002/cta

realizable using a single ICCII+, a single resistor R_1 and the two grounded capacitors in a similar topology to that given in [22] and using CCII−.

The voltage mode low-pass filter generated from the multiple feedback low-pass filter and using the FDNR–*C* circuit is shown in Figure 4(b). It has the same transfer function as given in Equation (3).

For a specified ω_0 and Q the design equations are given by

$$C_1 = C_2 = C \tag{4}$$

$$R_1 = \frac{2Q}{\omega_0 C} \quad \text{and} \quad R_2 = \frac{1}{2Q\omega_0 C} \tag{5}$$

The ω_0 and the Q passive sensitivities are given by

$$\underset{R_1}{\overset{\omega_0}{S}} = \underset{R_2}{\overset{\omega_0}{S}} = \underset{C_1}{\overset{\omega_0}{S}} = \underset{C_2}{\overset{\omega_0}{S}} = -\frac{1}{2} \tag{6}$$

$$\underset{R_1}{\overset{Q}{S}} = -\underset{R_2}{\overset{Q}{S}} = \frac{1}{2} \quad \text{and} \quad \underset{C_1}{\overset{Q}{S}} = -\underset{C_2}{\overset{Q}{S}} = -\frac{1}{2} + \frac{C_2}{C_1 + C_2} \tag{7}$$

For the equal C design, the Q sensitivities with respect to C_1 and C_2 are equal to zero.

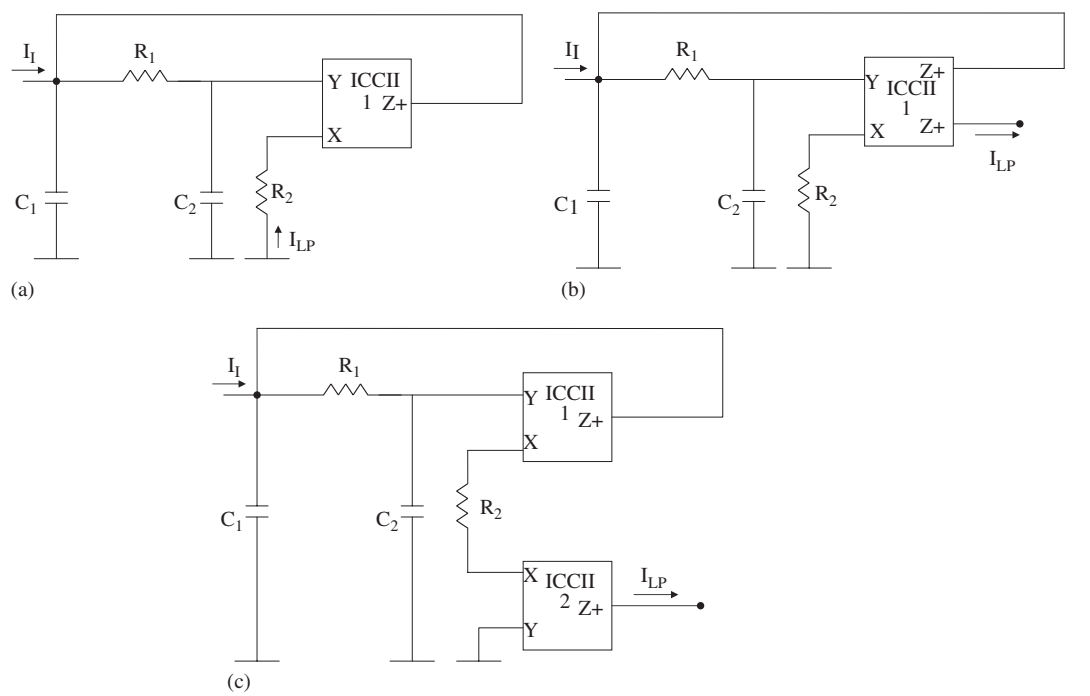

Figure 5. (a) Current mode low-pass filter generated from Figure 4(b) and using a single ICCII+; (b) grounded *C* current mode low-pass filter using double output ICCII+; and (c) grounded *C* current mode low-pass filter using two ICCII+.

DOI: 10.1002/cta

Figure 4(b) represents a high input impedance low-pass filter using the ICCII− in a similar way to the CCII− circuit in [23, 24]. It employs, however, one floating capacitor and its high-frequency limitations are worse than the circuit of Figure 4(a) as its numerator is affected by the ICCII− non-idealities as shown in Table IV.

The current mode grounded capacitor low-pass filter using a single ICCII+ is generated from the circuit of Figure 4(b) using the adjoint network theorem. It should be noted that the ICCII+ is represented by a voltage mirror (VM) between Y and X and a current mirror (CM) between X and Z+. When the adjoint network theorem is applied to Figure 4(b) the VM is replaced by a CM and the CM is replaced by a VM note that the ICCII+ is self-adjoint [2]. The input current is injected at the output voltage node $-V_{LP}$ and V_i is set to zero resulting in the output current I_{LP} flowing in R_2. Of course this output current cannot be used as its flowing in the grounded resistor R_2 and a second ICCII+ is needed as will be shown in the next section. The circuit current transfer function is given by

$$\frac{I_{LP}}{I_i} = \frac{1}{s^2 C_1 C_2 R_1 R_2 + s(C_1 + C_2)R_2 + 1} \tag{8}$$

Figure 5(b) represents the practical current mode low-pass filter obtained from Figure 5(a) and a double-output ICCII++ is used to obtain a high output impedance output node to deliver I_{LP}.

3. THE TWO CCII LOW-PASS FILTERS

3.1. The two ICCII+ current mode filters

Figure 5(c) represents another practical current mode low-pass filter using two single output ICCII+ to enable the delivery of the output current. The current transfer function is the same as given in Equation (8) and the design equations are given in Equations (4) and (5). This circuit has the disadvantage that the input impendence is not zero as desirable and is frequency dependent. It is interesting to see how the equivalent current mode circuits having zero input impedance from Figure 4(b) is generated.

3.2. The two ICCII+ voltage mode filters

Figure 6(a) is a high input impedance low-pass filter obtained from Figure 4(b) by adding an ICCII− at the input. A non-inverting low-pass response is obtained at port Y of the ICCII+ number 1, and an inverting response is available at terminal X of the same ICCII+. Notice that the current I entering port Z+ of the ICCII number 1 is the same as the current I entering port Z− of the second ICCII. Based on this observation the new circuit of Figure 6(b) can be generated from that of Figure 6(a). Since the Z+ terminal of the ICCII number 1 is not used then it can be changed to Z− as shown in Figure 6(b) resulting in a two ICCII− circuit.

3.3. The two CCII+ current mode filters

In this section a novel grounded C current mode low-pass filter using two single outputs CCII+ is generated from the circuit of Figure 6(b) by applying the adjoint network theorem. Set V_i to ground in the circuit of Figure 6(b) and inject I_i at the X terminal of ICCII number 1 (the output voltage $-V_{LP}$ node). The adjoint of the ICCII− is a CCII+ since the VM will be replaced by a

DOI: 10.1002/cta

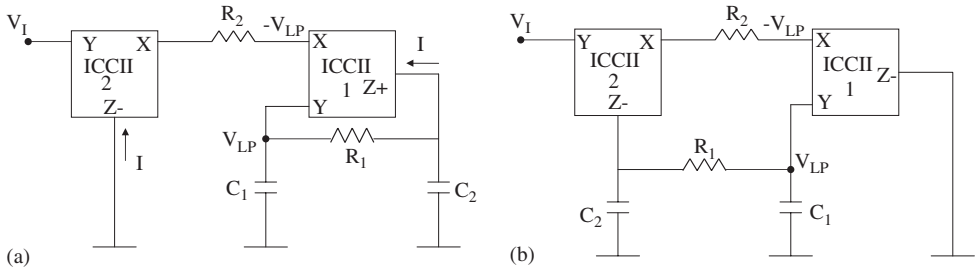

Figure 6. (a) A high input impedance grounded C voltage mode low-pass filter using one ICCII+ and one ICCII− and (b) equivalent high input impedance grounded C voltage mode low-pass filter using two ICCII−.

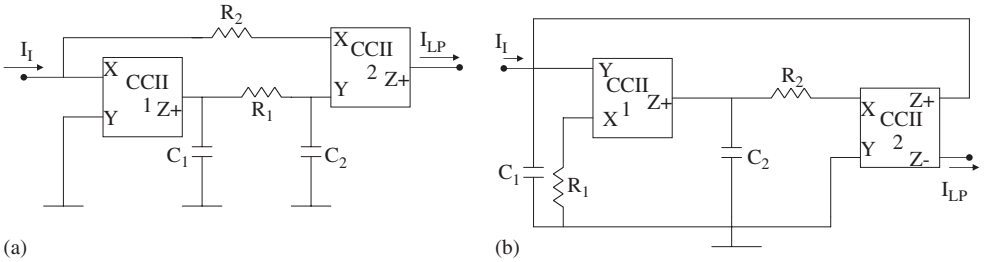

Figure 7. (a) Zero input impedance grounded C current mode low-pass filter using two CCII+ and (b) a non-zero input impedance grounded C current mode low-pass filter using two CCII+ [25].

CM [2] and the norator will be replaced by a nullator [6]. This CCII+ current mode low-pass filter is new to the best of the author's knowledge. Comparison of this circuit with a known grounded capacitor low-pass filter shown in Figure 7(b) [25] indicates the superiority of this circuit in having a zero input impedance and that it does not require a two-output CCII to deliver the output current.

3.4. The two ICCII− current mode filters

Since the adjoint of the ICCII− is the CCII+ and since it is desirable to generate new grounded capacitor low-pass filters using the ICCII−, therefore, one must find the proper voltage mode low-pass filter using two CCII+. Figure 8 represents such a well-known circuit [23, 26].

It is of interest to note that the topology of the circuit of Figure 8 is the same as that of the ICCII− voltage mode low-pass filter given in Figure 6(b). Of course not every CCII+ circuit results in an ICCII− circuit by just interchanging the CCII from one to another. However, only a special class of circuits has this property, and the circuits of Figures 6(b) and 8 are from this class. The application of the adjoint network theorem to the circuit of Figure 8 results in a new current mode low-pass filter shown in Figure 9(a), where I_i is injected at node X of the CCII+ number 1.

Another equivalent current mode low-pass filter is shown in Figure 9(b) which is obtained from Figure 6(b) by setting $V_i = 0$, inject I_i at the X terminal of the ICCII− number 2 and remove

DOI: 10.1002/cta

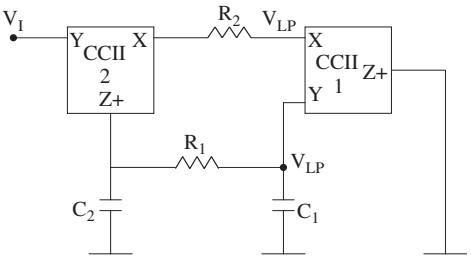

Figure 8. A high input impedance grounded C voltage mode low-pass filter using two CCII+ [23, 26].

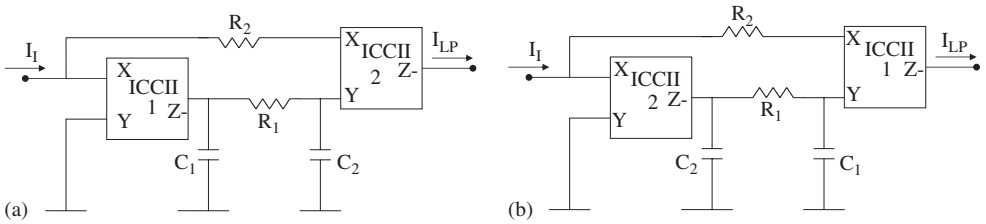

Figure 9. (a) Zero input impedance grounded C current mode low-pass filter using two ICCII− generated from Figure 8(a) using adjoint network theorem and (b) equivalent zero input impedance grounded C current mode low-pass filter using two ICCII generated from Figure 6(b).

ground from the Z− terminal of the ICCII− number 1 to obtain I_{LP}. Note that Figure 9(a) and (b) is generated from Figures 8 and 6(b), respectively, using two different methods and that is why both of them are included.

4. THE THREE ICCII+ LOW-PASS FILTERS

A new current mode low-pass filter using three ICCII+ is introduced in this section and shown in Figure 10. The circuit has all the advantages of the current mode low-pass filter of Figure 9(a) with the following two additional advantages. The first is that all passive elements are grounded; the second is that it has independent control over the filter Q by varying the resistor R without affecting ω_0.

The transfer function of the filter is given by

$$\frac{I_{LP}}{I_i} = \frac{1/C_1C_2R_1R_2}{s^2 + s/C_2R + 1/C_1C_2R_1R_2} \tag{9}$$

The ω_0 and Q are given by

$$\omega_0 = \frac{1}{\sqrt{C_1C_2R_1R_2}}, \quad Q = R\sqrt{\frac{C_2}{C_1R_1R_2}} \tag{10}$$

The circuit has very low passive sensitivities to all circuit components.

DOI: 10.1002/cta

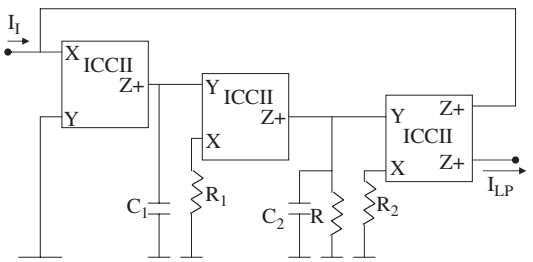

Figure 10. A new zero input impedance grounded C grounded R low-pass filter.

5. EFFECTS OF NON-IDEAL ICCII

At high frequencies, the ICCII is described by the matrix equation (1) where K and B are frequency dependent and are represented by the following equations:

$$K(s) = \frac{K_0}{1 + s/\omega_1} \tag{11}$$

$$B(s) = \frac{B_0}{1 + s/\omega_2} \tag{12}$$

where K_0 and B_0 are the DC values of $K(s)$ and $B(s)$, and they have magnitudes very close to one.

ω_1 and ω_2 are the 3 dB radian frequencies of $K(s)$ and $B(s)$, respectively.

Taking K and B of the ICCII as given in Equations (11) and (12), the denominator of the transfer function of the circuits of Figures 4(b), (c) and 9(a) are given, respectively, by

For the circuit of Figure 4(b):

$$D(s) = s^2 + s\frac{1}{R_1}\left(\frac{1}{C_1} + \frac{1}{C_2}\right) + \frac{KB}{C_1C_2R_1R_2} \tag{13}$$

For the circuit of Figure 4(c):

$$D(s) = s^2 + s\frac{1}{R_1}\left(\frac{1}{C_1} + \frac{1}{C_2}\right) + s\frac{1}{C_1R_2}(1 - K) + \frac{1}{C_1C_2R_1R_2} \tag{14}$$

For the circuit of Figure 9(a):

$$D(s) = s^2 + s\frac{1}{R_1}\left(\frac{1}{C_1} + \frac{1}{C_2}\right) + \frac{K_1B_2}{C_1C_2R_1R_2} \tag{15}$$

From the above $D(s)$ equations, the fractional shifts in ω_0 and Q for each of these filters can be calculated based on Budak–Petrela's method [19, 20]. The numerator of the transfer function and the fractional shifts in ω_0 and Q are given in Table IV, where ω_P is defined by

$$\frac{1}{\omega_P} = \frac{1}{\omega_1} + \frac{1}{\omega_2} \tag{16}$$

DOI: 10.1002/cta

Table IV also includes for comparison the results of the op amp circuits based on the op amp single pole model given by [19, 20]

$$A(s) = \frac{A_0}{1 + s/\omega_a} \tag{17}$$

From Table IV it is seen that the only two circuits having their numerator affected by the non-ideality of the active device are the op amp circuit of Figure 3(c) and the ICCII− low-pass filter of Figure 4(c). The ω_0 and Q are both affected by the non-ideality of the active device. It is seen, however, that the other ICCII circuits considered in Table IV have their ω_0 unaffected by the frequency-dependent K or B.

6. SIMULATION RESULTS

In this section Spice simulation results for most of the circuits included in this paper will be given. First, the three op amp circuits of Figure 3 are simulated using the μA 741 op amp from analog devices with $f_t = 1$ MHz and $f_a = 5$ Hz.

Figure 11(a) represents the magnitude and phase characteristics of the Sallen–Key filter designed to have a maximally flat magnitude (MFM) response, that is, $Q = 0.707$ and having f_0 of 1 MHz. The circuit components for equal R design are obtained as $R_1 = R_2 = 10\,\text{k}\Omega$, $C_1 = 22.5$ pF and $C_2 = 11.25$ pF.

Figure 11(b) represents the magnitude and phase characteristics of the inverting low-pass filter of Figure 3(b) designed with the same f_0 and Q as before. The circuit components for equal R design are obtained as $R_1 = R_2 = R_3 = 10\,\text{k}\Omega$, $C_1 = 33.77$ pF and $C_2 = 7.5$ pF.

Figure 11(c) represents the magnitude and phase characteristics of the non-inverting low-pass filter of Figure 3(c) designed with the same f_0 and Q as before.

The circuit components for equal C design are obtained as $C_1 = C_2 = 10\,\text{pF}$, $R_1 = 22.5\,\text{k}\Omega$, and $R_2 = 11.25\,\text{k}\Omega$. It is seen that non-infinity zeros for this circuit due to the finite gain bandwidth of the op amp as seen from Table IV degrade the magnitude and phase characteristics as seen from Figure 11(c) as compared with the ideal response.

It is seen from the op amp simulation results that it is not possible to realize low-pass responses with cut-off frequencies higher than 1 MHz.

Next Spice simulations for the current conveyor filter for $Q = 0.707$ and f_0 equal to 10 MHz are carried out using the CMOS ICCII of Figure 1(b) and (c) and the CCII+ of Figure 2 with aspect ratios given in Tables I–III.

Figure 12(a) represents the magnitude and phase characteristics of the low-pass filter of Figure 4(b) with the output taken at node Y of the ICCII+ of Figure 1(c) resulting in an inverting output response. The circuit components for equal C design are obtained as $C_1 = C_2 = 10$ pF, $R_1 = 2.25\,\text{k}\Omega$ and $R_2 = 1.125\,\text{k}\Omega$. It is seen that the magnitude characteristics coincides with that of the ideal response and there is a very small deviation in the phase characteristics.

Figure 12(b) represents the magnitude and phase characteristics of the high input impedance inverting low-pass filter of Figure 4(c). The passive circuit components are the same as in the previous circuit and the ICCII− of Figure 1(b) is used. It is seen that the finite zeros of the low-pass filter due to the non-unity and frequency-dependent B and K of the ICCII− as seen in Table IV degrades the characteristics at high frequencies.

DOI: 10.1002/cta

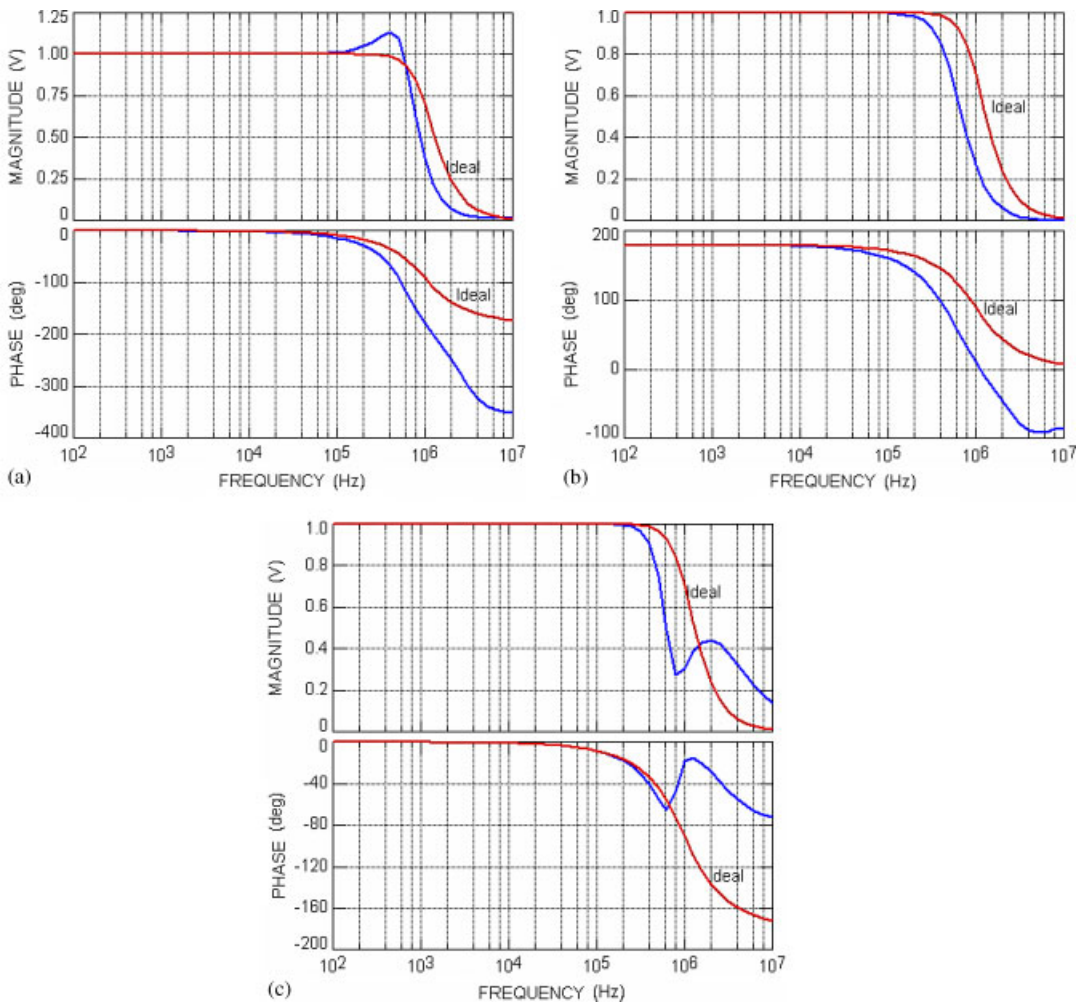

Figure 11. (a) Magnitude and phase characteristic of the circuit of Figure 3(a); (b) magnitude and phase characteristic of the circuit of Figure 3(b); and (c) magnitude and phase characteristic of the circuit of Figure 3(c).

Figure 12(c) represents the magnitude and phase characteristics of the current mode low-pass filter of Figure 5(b) simulated using the double output ICCII++ shown in Figure 1(c). The passive circuit components are the same as in the previous circuit. It is seen that the magnitude characteristics coincides with that of the ideal response and there is a very small deviation in the phase response.

Figure 13 represents the magnitude and phase characteristics of the voltage mode non-inverting low-pass filter of Figure 6(b) with the output taken as the non-inverting one. The simulation results indicate a slight increase in magnitude response due to the non-ideal ICCII−, which results in a slight increase in the filter Q.

DOI: 10.1002/cta

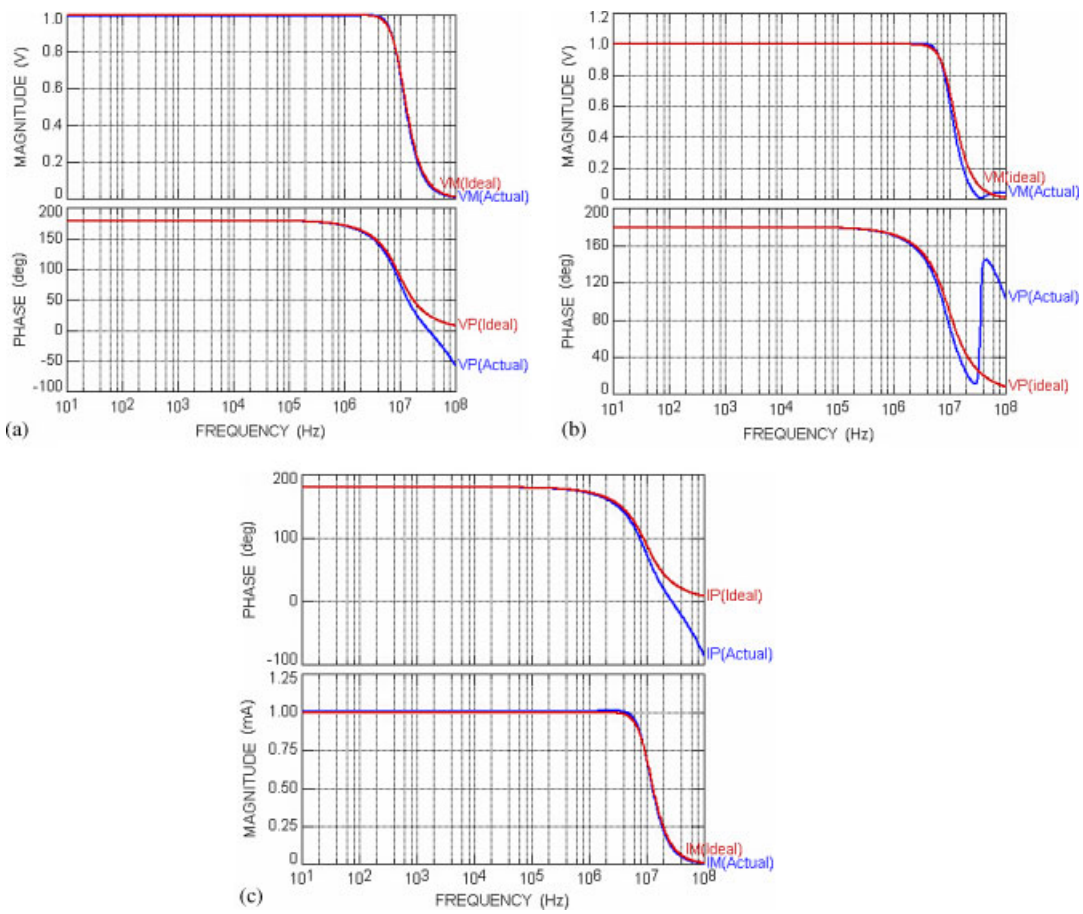

Figure 12. (a) Magnitude and phase characteristic of the circuit of Figure 4(b); (b) magnitude and phase characteristic of the circuit of Figure 4(c); and (c) magnitude and phase characteristic of the circuit of Figure 5(b).

To examine the CCII+ current mode filter of Figure 7(a) a MFM low-pass filter with the same specifications as before is designed. Figure 14 represents the magnitude and phase characteristics obtained from the Spice simulations using the CMOS CCII+ shown in Figure 2. The results are very close to the ideal MFM response.

The new current mode filter of Figure 9(a) using two ICCII− is designed to realize a MFM response having $f_0 = 10$ MHz with the same resistor and capacitor values as before. Figure 15 represents the magnitude and phase characteristics obtained from the Spice simulations using the CMOS ICCII− shown in Figure 1(b).

Figure 16 represents the magnitude and phase characteristics of the low-pass filter of Figure 10 using three CCII++ of Figure 1(c). The circuit components are obtained as $C_1 = C_2 = 10$ pF, $R_1 = R_2 = 1.59\,\text{k}\Omega$ and $R = 1.125\,\text{k}\Omega$. It is seen that the magnitude characteristics coincides with that of the ideal response and there is a very small deviation in the phase characteristics.

DOI: 10.1002/cta

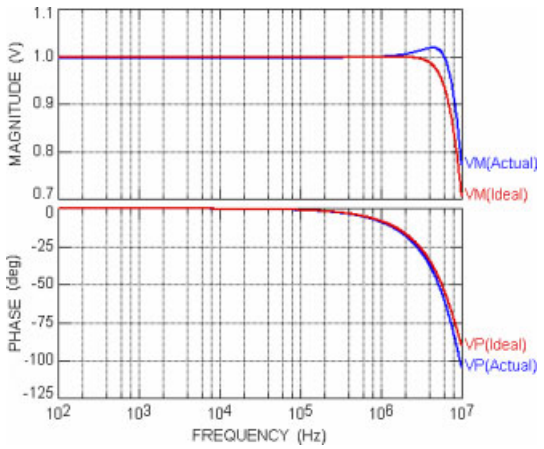

Figure 13. Magnitude and phase characteristic of the circuit of Figure 6(b).

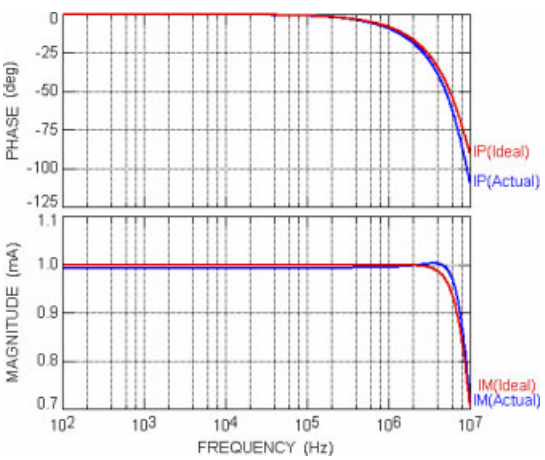

Figure 14. Magnitude and phase characteristic of the circuit of Figure 7(a).

7. CONCLUSIONS

Three new grounded capacitor current mode low-pass filters using two inverting CCII are given. The circuits employ the minimum number of passive circuit components, namely two resistors and two capacitors. The circuits are generated from three new voltage mode low-pass filters realized with the ICCII. A new grounded capacitor CCII+ current mode low-pass filter is also introduced. This new current mode low-pass filter is superior to all previously known two CCII+ current mode low-pass filters since it has zero input impedance. A new grounded passive components low-pass filter with independent control on Q and using three ICCII+ is also introduced. The non-ideal analysis of the ICCII circuits is summarized and compared with the op amp low-pass filters in Table IV.

DOI: 10.1002/cta

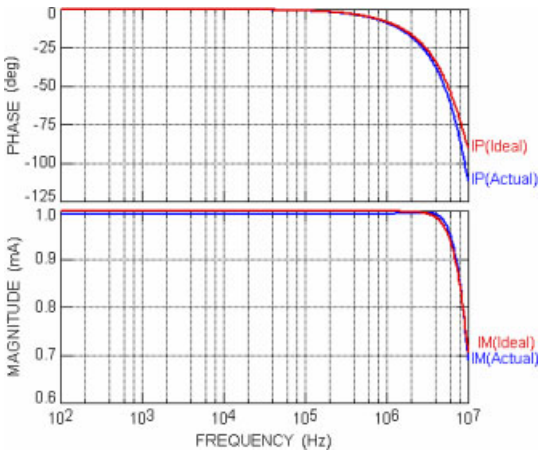

Figure 15. Magnitude and phase characteristic of the circuit of Figure 9(a).

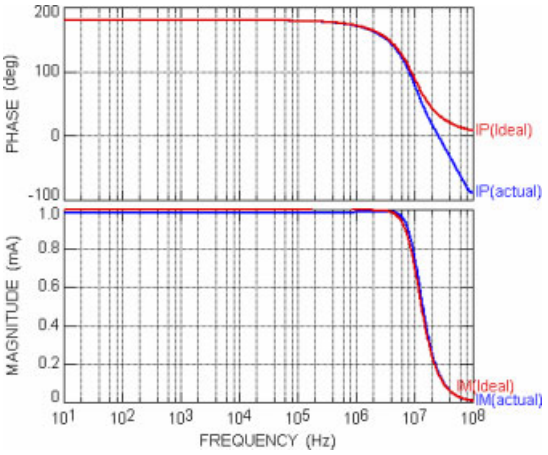

Figure 16. Magnitude and phase characteristic of the circuit of Figure 10.

Spice simulation results based on using the 0.5 μm CMOS model are included to support the theoretical analysis. The non-ideal analysis of the ICCII circuits is summarized and compared with the op amp low-pass filters in Table IV.

It is worth noting that it is not the intention of this paper to conclude that the ICCII+ or the ICCII− is better than the CCII+ or the opposite; they are completing each other in the current conveyor family [27]. Since the ICCII− and the CCII+ are adjoint to each other and the ICCII+ is self-adjoint this will lead to the generation of new circuits from known ones.

DOI: 10.1002/cta

REFERENCES

1. Sedra AS, Smith KC. A second generation current conveyor and its applications. *IEEE Transactions on Circuit Theory* 1970; **132**:132–134.
2. Awad IA, Soliman AM. The inverting second generation current conveyors: the missing building blocks, CMOS realizations and applications. *International Journal of Electronics* 1999; **84**:413–432.
3. Elwan HO, Soliman AM. Novel CMOS differential voltage current conveyor and its applications. *IEE Proceedings—Circuits Devices and Systems* 1997; **144**:195–200.
4. Chiu W, Liu SI, Tsao HW, Chen JJ. CMOS differential difference current conveyors and their applications. *IEE Proceedings—Circuits Devices and Systems* 1996; **143**:91–96.
5. El-Adawy AA, Soliman A, Elwan HO. A novel fully differential current conveyor and applications for analog VLSI. *IEEE Transactions on Circuits and Systems II* 2000; **47**:306–313.
6. Lopez-Martin AJ, Ramirez-Angulo J, Carvaial RG. A proposal for high performance CCII-based analogue CMOS design. *International Journal of Circuit Theory and Applications* 2005; **33**:379–391.
7. Soliman AM. Generalized voltage and current conveyors: practical realizations using CCII. *IEICE Transactions on Fundamentals of Electronics, Communications and Computer Sciences* (*Japan*) 1998; **E81**:973–975.
8. Cajka J, Dostal T, Vrba K. General view on current conveyors. *International Journal of Circuit Theory and Applications* 2004; **32**:133–138.
9. Roberts GW, Sedra AS. All current-mode selective circuits. *Electronics Letters* 1989; **25**:759–761.
10. Carlosena A, Moschytz GS. Nullators and norators in voltage to current mode transformations. *International Journal of Circuit Theory and Applications* 1993; **21**:421–424.
11. Gunes EO, Anday F. Realization of current mode universal filter using CFCCIIs. *Electronics Letters* 1996; **32**:1081–1082.
12. Ozoguz S, Acar C. Universal current mode filter with reduced number of active and passive components. *Electronics Letters* 1997; **33**:948–949.
13. Ozoguz S, Toker A, Cicekoglu O. High output impedance current mode multifunction filter with minimum number of active and reduced number of passive elements. *Electronics Letters* 1998; **34**:1807–1809.
14. Minaei S, Sayin OK, Kuntman H. A new CMOS electronically tunable current conveyor and its application to current mode filters. *IEEE Transactions on Circuits and Systems I* 2006; **53**:1448–1457.
15. Bhusan M, Newcomb RW. Grounding of capacitors in integrated circuits. *Electronics Letters* 1967; **3**:148–149.
16. Souliotis G, Psychalinos C. Harmonic oscillators realized using current amplifiers and grounded capacitors. *International Journal of Circuit Theory and Applications* 2007; **35**:165–173.
17. Surakampontorn W, Riewruja V, Kumwachara K, Dejhan K. Accurate CMOS based current conveyors. *IEEE Transactions on Instrumentation and Measurement* 1991; **40**:699–702.
18. Van Valkenburg ME. *Analog Filter Design*. Holt Rinehart and Winston: New York, 1982.
19. Budak B, Petrala D. Frequency limitations of active filters using operational amplifiers. *IEEE Transactions on Circuit Theory* 1972; **19**:322–328.
20. Budak A. *Passive and Active Network Analysis and Synthesis*. Houghton Mifflin: New Jersey, 1974.
21. Soliman AM. A new single operational amplifier active RC band-pass network with reduced sensitivity to amplifier gain-bandwidth product. *International Journal of Circuit Theory and Applications* 1978; **6**:321–326.
22. Soliman AM. Ford–Girling equivalent circuit using CCII. *Electronics Letters* 1978; **14**:721–722.
23. Soliman AM. Generation of current conveyor based low-pass filters from passive RLC filter. *Journal of the Franklin Institute* 1998; **335B**:1283–1297.
24. Liu SI, Tsao HW. Single CCII biquads with high input impedance. *IEEE Transactions on Circuits and Systems* 1991; **38**:456–461.
25. Soliman AM. New current mode filters using current conveyors. *Archiv fur Elektronik und Ubertragungstechnik AEU* 1997; **51**:275–278.
26. Fabre A, Dayoub F, Duruisseau I, Kamoun M. High input impedance insensitive second order filters implemented from current conveyors. *IEEE Transactions on Circuits and Systems* 1994; **41**:918–921.
27. Soliman AM. Voltage mode and current mode Tow Thomas bi-quadratic filters using inverting CCII. *International Journal of Circuit Theory and Applications* 2007; **35**:463–467.

DOI: 10.1002/cta